

Evaluation of SAR in a human body model due to wireless power transmission in the 10 MHz band

Ilkka Laakso¹, Shogo Tsuchida¹, Akimasa Hirata¹, Yoshitsugu Kamimura²

1: Nagoya Institute of Technology, Department of Computer Science and Engineering, Japan

2: Utsunomiya University, Japan

Corresponding Author: Akimasa Hirata

Address: Nagoya Institute of Technology, Gokiso-cho, Showa-ku, Nagoya 466-8555, Japan

Tel&Fax: +81-52-735-7916

E-mail: ahirata@nitech.ac.jp

Abstract

This study discusses a computational method for calculating the specific absorption rate (SAR) due to a wireless power transmission system in the 10 MHz frequency band. A two-step quasi-static method comprised of the method of moments and the scalar potential finite difference method is proposed. The applicability of the quasi-static approximation for localized exposure in this frequency band is discussed by comparing the SAR in a lossy dielectric cylinder computed with a full-wave electromagnetic analysis and the quasi-static approximation. From the computational results, the input impedance of the resonant coils was affected by the existence of the cylinder. On the other hand, the magnetic field distribution in free space and that considering the cylinder and an impedance matching circuit were in a good agreement; the maximum difference in the amplitude of magnetic field was 4.8%. For a cylinder-coil distance of 10 mm, the difference between the peak 10 g averaged SAR in the cylinder computed with the full-wave electromagnetic method and our quasi-static method was 7.8%. These results suggest that the quasi-static approach is applicable for conducting the dosimetry of wireless power transmission in the 10 MHz band. With our two-step quasi-static method, the SAR in the anatomically based model was computed for different exposure scenarios. From those computations, the allowable input power satisfying the limit of a peak 10 g averaged SAR of 2.0 W/kg was 830 W in the worst case exposure scenario with a coil positioned at a distance of 30 mm from the chest.

1. Introduction

A pilot study realizing a wireless power transmission system with magnetically coupled coils was conducted by Kurs *et al.* (2007). Attention is needed on the human safety of radio waves used in such systems because the expected power transmission is much larger than that used in wireless communications. In particular, the maximum allowable input power that satisfies human exposure limits prescribed in international safety guidelines/standards (ICNIRP 1998, IEEE 2005) must be determined. One of the frequency bands considered for wireless power transmission is the range of a few dozen megahertz. Particularly, a frequency of 13.56 MHz would be promising for this application, since it has been assigned for industrial, scientific and medical use.

For frequencies above 10 MHz, the human exposure limits are defined in terms of the specific absorption rate (SAR). For localized exposure, the SAR averaged over 10 g of tissue is used, while the whole-body averaged SAR is used for whole-body exposure. Kurs *et al.* (2007) briefly discussed the compliance of wireless power transmission by calculating the amplitudes of the magnetic and electric fields between the coupled coils when transferring a power of 60 W across 2 m. However, the calculated electric/magnetic field strengths did not satisfy the reference level in the ICNIRP guidelines (1998). In that case, the local and whole-body SARs (basic restrictions) should be evaluated for assessing the compliance with the guidelines.

Kurs *et al.* (2007) suggested that two magnetic resonance modes exist while no information is given on which of the two modes was considered in that study. Hirayama *et al.* (2009) conducted a detailed analysis of the two transmitting modes and then referred to these two modes as odd and even, corresponding to the lower and higher frequency modes, respectively. This naming scheme originates from the similarity of the generated magnetic field distribution with the electric field distribution of a small dipole. Hirayama *et al.* (2009) also suggested that

the even mode resonance could be useful for reducing undesirable emissions and giving a higher efficiency. It would be worth investigating the induced field in the human body for these two modes from the standpoint of human protection from electromagnetic fields.

Christ *et al.* (2011) conducted dosimetry for wireless power transmission at 8 MHz with the finite-difference time-domain (FDTD) method. However, a detailed explanation was not given, especially for which mode was considered. Although the FDTD method is a very powerful method for solving for the EM interaction with biological tissue, a high-resolution analysis is time consuming especially at lower frequencies and for curved structures. Note that the above-mentioned two resonance frequencies are close to each other, and thus some discrepancy in the computational modelling may result in an error in the resonance frequencies.

Park *et al.* (2011) conducted dosimetry with a two-step approach based on a quasi-static approximation. First, the finite-element method (FEM) was used to compute the magnetic field generated by the magnetically coupled coils (Jin 2002). Then, dosimetry was conducted with the impedance method (Orcutt and Gandhi 1988) by considering the current distribution as a source. However, the transfer efficiency of the system considered was at most 30% or not strongly-coupled. In addition, the validity of the approach was not verified by comparing the results to a full-wave electromagnetic analysis. Furthermore, the input impedance of the coil or the resonance frequencies could be altered by the existence of the human body (Kurs *et al.* 2007), which was not discussed in that study. Feliziani and De Santis (2011) investigated the effectiveness of the quasi-static approximation for wireless power transmission in implanted medical devices. A homogeneous sphere was considered as a model for the human body. It was then concluded that the presence of biological tissue does not significantly alter the magnetic coupling performances for frequencies at least up to a few megahertz.

In this study, we first investigate the input impedance and resonance frequencies of

magnetically coupled coils with and without a human-sized lossy dielectric cylinder placed in proximity of the coils using full-wave analysis. The local SAR in the cylinder computed with full-wave analysis and our two-step method based on the quasi-static approximation are compared to verify the effectiveness of our proposal. Finally, the SAR in an anatomically based model is evaluated for different exposure scenarios in order to estimate the maximum allowable transmission power of the system.

2. Model and methods

2.1. Human body models

In the preliminary investigation of the quasi-static approximation, a simple homogeneous cylindrical human model was considered. The height and diameter of the cylinder were chosen as 1.7 m and 0.14 m, respectively, approximately corresponding to the size of an adult human. The dielectric properties of the cylinder were $2/3$ that of muscle, which is representative of the average electrical properties over the human body. Realistic computation of SAR values employed the Japanese male whole-body model TARO (Nagaoka *et al.* 2004). The model consists of cubical voxels with a side length of 2 mm. The dielectric properties of tissues were taken from Gabriel *et al.* (1996).

2.2. Full-wave analysis

The electromagnetic full-wave analysis was carried out using the commercial software FEKO (2011), which uses the method of moments (MoM) coupled with the FEM. The MoM (Gibson 2007) was used for modelling the resonant coils, while the FEM was used for modelling the fields inside the human phantom. FEKO is often used for human-RF interactions, and its effectiveness has been confirmed in several studies (e.g., Bottomley *et al.* 2010, Ikeuchi and

Hirata 2011). The FDTD method is often applied to dosimetry at radio frequencies. However, that method was not used here, as it is difficult to represent curved resonant coils, which would result in errors in resonant modes and frequencies (section 2.4).

2.3. Quasi-static analysis

Electromagnetic field exposure can be decoupled into electric and magnetic field exposure when the quasi-static approximation is valid. In the quasi-static approximation, the displacement current is ignored and the external magnetic field/source current distribution is considered not to be perturbed by the existence of the human body. Because the quasi-static approximation simplifies the computational procedure dramatically, this approximation is often used in dosimetry at extremely low frequencies (e.g., Dimbylow 1998, Nishizawa *et al.* 2004, Wu *et al.* 2007). Note that the upper frequency, where the quasi-static approximation is valid, is shown to be approximately 10 MHz for the dosimetry of contact currents (Hirata *et al.* 2011). In this study, the quasi-static approximation is applied for calculations of the SAR due to wireless power transmission in the 10 MHz band. The proposed computational method consists of two main steps: first, the source current/vector potential is determined, and then, the induced electric field and SAR in the body are calculated. A similar two-step method has been used previously at lower frequencies (Wu *et al.* 2007, Park *et al.* 2011). The SAR computed by the two-step method will be compared to that computed by full-wave analysis to confirm the applicability of the quasi-static approximation in the 10 MHz band.

In the proposed two-step method, the surface current distribution on the coupled coils is first obtained using the MoM (FEKO) without considering the human body. Next, assuming that the human body does not disturb the current distribution of the coils, the magnetic vector potential is determined for each voxel in the human body model. The induced electric field is then computed by solving the scalar potential finite difference (SPFD) equation system numerically

(Dawson 1996). Finally, the SAR in each voxel is calculated from the electric field by the ‘mid-ordinate algorithm’ (Laakso *et al* 2010), i.e., the average electric field at the centre point of the voxel is calculated from the twelve edges of the voxel. The absolute value of the average is then squared, multiplied by the conductivity, and divided by the mass density. The spatially-averaged SAR is determined by averaging the voxel SAR over 10 g cubical volumes as described in IEEE (2002).

Compared to full-wave analysis (e.g. the FDTD method), in the two-step method, the source current distribution (and the resulting vector potential) needs to be solved only once for a single system configuration, while the surrounding air region does not need to be modelled. This leads to a greatly reduced computational effort, especially when studying a variety of different human body models/human-coil positions.

2.4. Modelling resonant coils

Figure 1 illustrates the geometry of the wireless power transmission system, consisting of two resonant coils. In FEKO, the coils were modelled as perfectly conducting wires with a diameter of 2 mm and the system was excited by a voltage source located at port 1. Coil dimensions suggested by Hirayama *et al.* (2009) were used; the radius of the coil was 300 mm, and the number of turns was five. The separation between the coils was 300 mm. Unlike in Hirayama *et al.* (2009), one-loop coils for feeding and receiving power were not considered as they are not essential for the field distribution (Amano *et al.* 2011). For these parameters, two resonances frequencies of 11.36 MHz (odd mode) and 11.92 MHz (even mode) were observed. The magnetic field distributions of the two transmission modes are shown in figure 2.

3. Computational results

3.1. Input impedance of coils and power transmission efficiency

The effect of the presence of the human body on the input impedance and power transmission efficiency of the system was investigated by placing the lossy dielectric cylinder in proximity of the coils at the position defined in figure 1. The reason for choosing this position is that the coils and the cylinder are located closest to each other, resulting in the largest variation of the input impedance of the coils. Figure 3 shows the power transmission efficiency of the system with and without the cylinder computed using FEKO. Without the cylinder, at the odd-mode (11.36 MHz) and even-mode (11.92 MHz) resonance frequencies, the power transmission efficiencies were 99.5% and 99.9%, respectively. With the cylinder, the resonance frequencies shifted to 11.10 MHz and 11.54 MHz, respectively. However, from the standpoint of spectrum management, instead of using a different transmission frequency, the input impedance of the coils could be adjusted by an active circuit to keep the transmission frequencies constant. When the impedance was matched with appropriate capacitances at 11.36 MHz and 11.92 MHz, the power transmission efficiencies were 95.9% and 94.6%, respectively.

3.2. Quasi-static approximation compared to full-wave analysis

In order to confirm the validity of the two-step computational method based on the quasi-static approximation, we compared the magnetic and electric field distributions with and without the dielectric cylinder. With the cylinder, the input impedance was matched as described in section 3.1. Figure 4 shows the magnetic and electric field distributions on the mid-horizontal cross section of the lossy cylinder calculated using FEKO for the odd mode. Qualitatively similar results were also observed for the even mode, although not shown here in order to avoid repetition. As shown in figures 4(a) and (b), the magnetic field distributions with and without the cylinder were in good agreement. The maximum difference over the whole cylinder

normalized by the maximum magnetic field was 4.8%. On the contrary, as shown in figures 4 (c) and (d), the electric field distribution was disturbed due to the existence of the cylinder, because the human body is a conductor at low frequencies. The perturbed electric field is the primary reason for the change in the input impedance observed in section 3.1. However, the external electric field does not significantly penetrate into the cylinder; thus, it has a minor effect on the SAR, as shown below. With the quasi-static approximation, the effect of the external electric field is ignored, because there is no displacement current.

The SAR computed with the full-wave analysis (FEKO) and the quasi-static approach were compared for the two transmission modes when the input power was 1 W. At the lower resonance frequency (odd mode), peak 10 g SARs computed with the full-wave analysis and our quasi-static approach were 3.34 mW/kg and 3.14 mW/kg, respectively. At the higher resonance frequency (even mode), peak 10 g SARs computed with full-wave analysis and the quasi-static approach were 4.37 mW/kg and 4.03 mW/kg, respectively. The difference in the peak SAR between FEKO and the quasi-static approach decreased from 7.8% to 4.2% as the distance between the cylinder and the coils was increased from 10 mm to 50 mm.

The decreasing difference between the full-wave analysis and the quasi-static approximation with distance can be attributed to the effect of the external electric field, which was not considered in the quasi-static approximation. In addition, some of the difference is caused by the use of different numerical grids in FEKO and in our SPFD solver. Our SPFD solver used a uniform 2 mm cubical grid while FEKO employed a variable-sized mesh consisting of tetrahedral elements. The size of the smallest tetrahedron was no less than 10 mm due to limitations in computational memory. Nonetheless, the differences between the full-wave analysis and the quasi-static approximation were smaller than those reported in an interlaboratory comparison of SAR values calculated by the FDTD method at 5-10% for

whole-body exposure (Dimbylow *et al.* 2008) and 30% for localized exposure (Beard *et al.* 2006). These results suggest that the quasi-static approximation is reasonably applicable even in this frequency band.

3.3. SAR in anatomically based model

The quasi-static approach was used for calculating the SAR values in the anatomically realistic body model TARO for different coil positions. All SAR values were normalized to an input power of 1 W. Figures 5, 6, and 7 show the peak 10 g averaged SAR for different coil positions with respect to the body model. The whole-body averaged SAR is not shown, because it was less restricting when compared to the basic restriction limits in almost all the studied positions (see below). The lateral position (figure 5), the height of the coils (figure 6), and the distance between the body and the coil (figure 7) were varied. Note that the closest horizontal distance between the nose tip of the model and the coils is 10 mm, or 30 mm between the chest of the model and the coils.

Similarly to the cylindrical model, the peak SAR values are greater for the even mode in almost all of the studied positions. This is because the odd-mode magnetic field is less localized than that of the even mode. The largest peak SAR values occur when the human body is located directly in front of either of the coils, the height of the coil is in front of the chest, and the distance to the coil is as close as possible. The distribution of the SAR and the direction of the induced current in this worst-case exposure condition for the even and odd modes are shown in figures 8 (a) and (b), respectively. The highest SAR values are located in the muscle tissue in the chest at a depth of around 10–20 mm.

When compared to the basic restriction limits of a peak 10 g SAR of 2 W/kg and a whole-body averaged SAR of 0.08 W/kg (IEEE 2005), the limit of the 10 g averaged SAR is more restrictive

than that of the whole-body averaged SAR for human-coil distances shorter than 150 mm (except in positions G and H in figure 6). In the worst-case exposure condition, the maximal allowable input power that satisfies the basic restriction limit is 830 W for the even mode and 1100 W for the odd mode. However, as figure 7 shows, the peak 10 g averaged SAR decreases rapidly when the distance between the coils and the human body increases. For instance, for human-coil distances of 50 mm, 100 mm, or 150 mm, the allowable input powers would be 2.0 kW, 4.9 kW, or 11 kW, respectively.

4. Summary

The present study proposed a two-step computational method for calculating the induced field in the human body due to a wireless power transmission system in the 10 MHz band. The method, comprised of the MoM and the SPFD methods, is based on the quasi-static approximation. For validation, the proposed method and a full-wave electromagnetic method were used for determining the SAR in an exposure scenario that consisted of a lossy dielectric cylinder placed in proximity of the power transmission system. The input impedance of the resonant coils was altered by the existence of the cylinder, which can be attributed to the perturbed electric field. However, when the impedance mismatch was adjusted by adding appropriate capacitances, the magnetic field of the system was only slightly perturbed by the cylinder, and the SAR values calculated with the quasi-static approach and the full-wave analysis were in good agreement. These results suggest that the quasi-static approach is reasonably accurate for the dosimetry of wireless power transmission even in the 10 MHz band.

Compared to full-wave analysis, the two-step quasi-static approach has the advantage of a greatly reduced computational cost. For example, the computational time required for obtaining the full-wave solution in the lossy cylinder was 12 h on a workstation using the FEKO software.

On the contrary, the time needed for computing the surface current on the coils and the resulting magnetic vector potential distribution in free space was 1 hour (first step). Then, the time for computing the induced electric field from the SPFD equation in the anatomically based model for each coil position was just a few minutes (second step). Finally, the SAR was calculated from the electric field.

The SAR in an anatomically based human model was computed for different scenarios using the quasi-static approach. When compared with the basic restriction limits in the international guidelines (IEEE 2005), the limit for the local 10 g averaged SAR was more restrictive than that for the whole-body averaged SAR. In addition, the even mode operation provided a higher local SAR than the odd mode operation. Since the distance between the coils considered here was 300 mm for realizing high transmission efficiency, the human body model could not be positioned between the coils. Thus, a different conclusion might be obtained for a longer transmission distance. In the worst case exposure scenario considered herein, with either of the resonant coils located directly in front of the chest, the maximum allowable input power that satisfied the peak 10 g averaged SAR limit of 2.0 W/kg was 830 W. However, the maximum allowable power rose very steeply when the distance between the coil and the human body increased. Consequently, for potential applications, where the power transmission could be as high as 10 kW (Shinohara 2011), compliance with the exposure guidelines could be established by defining a short safety distance, e.g., 150—200 mm for a power transmission of 10 kW.

Acknowledgement

The authors would like to thank Prof. Hiroshi Hirayama (Nagoya Institute of Technology) for helpful discussion on magnetically-coupled coils. The authors wish to thank the Academy of Finland and the Finnish Cultural Foundation for financial support.

References

- Amano T, Hirayama H, Kikuma N, and Sakakibara K 2011 A consideration of helical antenna for wireless power transmission *Proc. IEICE Society Conf.* B-1-14
- Beard B B, Kainz W, Onishi T, Iyama T, Watanabe S, Fujiwara O, Wang J, Bit-Babik G, Faraone A, Wiart J, Christ A, Kuster N, Lee A-K, Koeze H, Siegbahn M, Keshvari J, Abrishamkar H, Simon W, Manteuffel D, and Nikoloski N 2006, Comparisons of computed mobile phone induced SAR in the SAM phantom to that in anatomically correct models of the human head *IEEE Trans. Electromagnet. Compat.* **48** 397-407
- Bottomley P A, Kumar A, Edelstein W A, Allen J M, Karmarkar P V 2010 Designing passive MRI-safe implantable conducting leads with electrodes *Med. Phys.* **37** 3828-43
- Christ A, Douglas M G, Roman J, Cooper E B, Sample A P, Smith J R, Kuster N 2011 Numerical Electromagnetic Analysis of Human Exposure for Wireless Power Transfer Systems *Proc. Int'l Conf. European BioElectromagnetic Association 2011*
- Dawson T W and Stuchly M A 1996 Analytic validation of a three-dimensional scalar-potential finite-difference code for low-frequency magnetic induction *Appl. Comput. Electromagnet. Soc. J.* **11** 63-71
- Dimbylow P 1998 Induced current densities from low-frequency magnetic fields in a 2 mm resolution, anatomically realistic model of the body *Phys. Med. Biol.* **43** 221
- Dimbylow P, Hirata A, and Nagaoka T, 2008 Intercomparison of whole-body averaged SAR in European and Japanese voxel phantoms *Phys. Med. Biol.* **53** 5883-97
- FEKO 2011 Electromagnetic Software and Systems (EMSS). [Online]. Available: <http://www.feko.info/>
- Feliziani M and De Santis V 2011 Magnetic field analysis and lumped inductance extraction for wireless power transfer in implanted medical devices *Proc. Asia-Pacific Electromagnetic*

Compat. T-We3-1

Gabriel S, Lau R W, and Gabriel C 1996 The dielectric properties of biological tissues: III.

Parametric models for the dielectric spectrum of tissues *Phys. Med. Biol.* **41** 2271-93

Gibson W C 2007 The method of moments in electromagnetics, Chapman and Hall/CRC

Hirata A, Hattori J, Fujiwara O, and Suzuki Y 2011 Computational uncertainty of induced electric field in human body due to contact current *Proc. Int'l Conf. European BioElectromagnetic Association 2011*

Hirayama H, Ozawa T, Kikuma N, and Sakakibara N 2009 A consideration of electro-magnetic-resonant coupling mode in wireless power transmission *IEICE Electron. Express.* **6** 1421-5

Ikeuchi R and Hirata A 2011 Dipole antenna above EBG substrate for local SAR reduction *IEEE Antenna Wirel. Propag. Lett.* **10** 904-6

ICNIRP 1998 Guidelines for limiting exposure to time-varying electric, magnetic, and electromagnetic fields (up to 300 GHz) *Health Phys.* **74** 494-522

IEEE 2002 IEEE recommended practice for measurements and computations of radio frequency electromagnetic fields with respect to human exposure to such fields, 100 kHz–300 GHz (C95.3)

IEEE 2005 IEEE standard for safety levels with respect to human exposure to radio frequency electromagnetic fields, 3 kHz to 300 GHz (C95.1)

Jin J M 2002 The finite element method in electromagnetics, 2nd Ed, Wiley-IEEE Press

Kurs A, Karalis A, Moffatt R, Joannopoulos J D, Fisher P, and Soljacic M 2007 Wireless power transfer via strongly coupled magnetic resonance *Science* **317** 83-6

Laakso I, Uusitupa T and Ilvonen S 2010 Comparison of SAR calculation algorithms for the finite-difference time-domain method *Phys. Med. Biol.* **55** N421-31

Nagaoka T, Watanabe S, Sakurai K, Kunieda E, Watanabe S, Taki M and Yamanaka Y 2004 Development of realistic high-resolution whole-body voxel models of Japanese adult males

and females of average height and weight, and application of models to radio-frequency electromagnetic-field dosimetry *Phys. Med. Biol.* **49** 1-15

Nishizawa S, Ruoss H-O, Landstorfer F M and Hashimoto O 2004 Numerical study on an equivalent source model for inhomogeneous magnetic field dosimetry in the low-frequency range *IEEE Trans. Biomed. Eng.* **51** 612-6

Orcutt N and Gandhi O P 1988 A 3-D impedance method to calculate power deposition in biological bodies subjected to time varying magnetic fields *IEEE Trans. Biomed. Eng.* **35** 577-83

Park S W, Wake K, Watanabe 2011 Preliminary study of dosimetry for wireless power transfer system using a magnetic resonance coupling *Proc. Int'l Conf. European BioElectromagnetic Association 2011* (Dosimetry 4th talk)

Shinohara N 2011 Power without wires *IEEE Microwave Magazine* **12** S64-73

Wu D, Qiang R, Chen J, Seldman S, Witters D, and Kainz W 2007 Possible overexposure of pregnant women to emissions from a walk through metal detector *Phys. Med. Biol.* **52** 5735-48

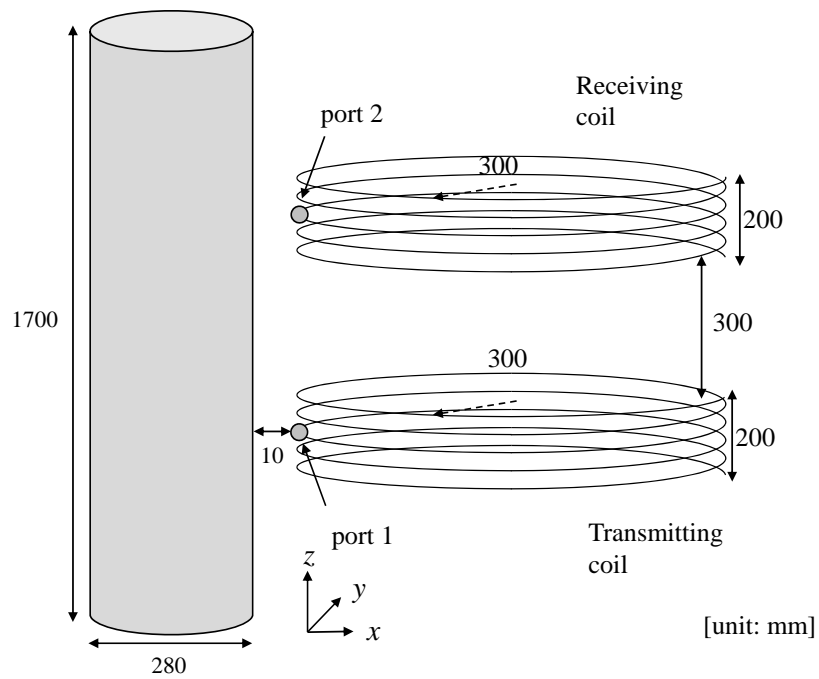


Figure 1. The geometry of the coils and the exposure conditions with the lossy dielectric cylinder.

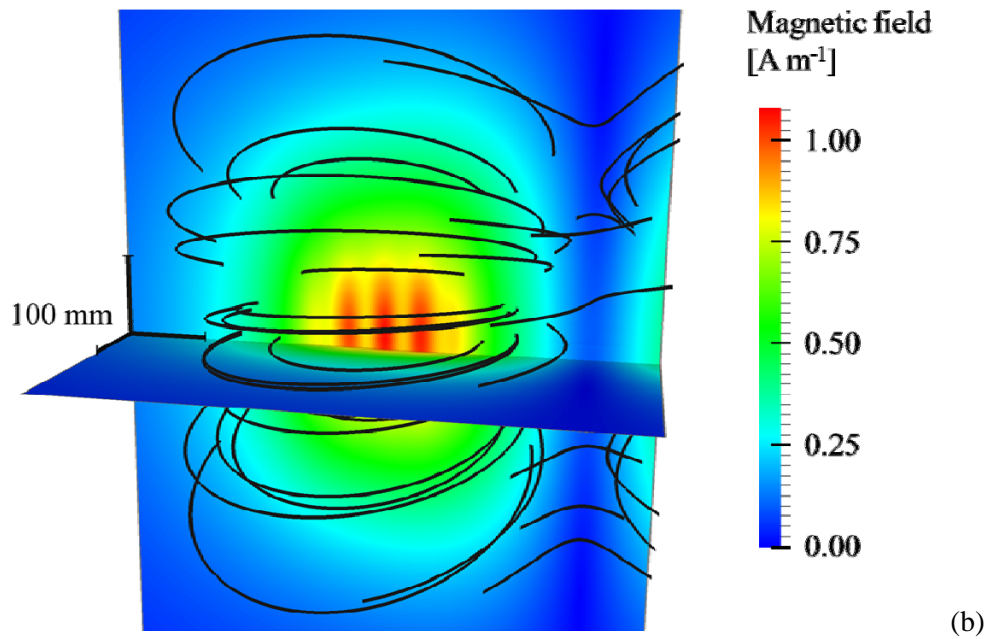
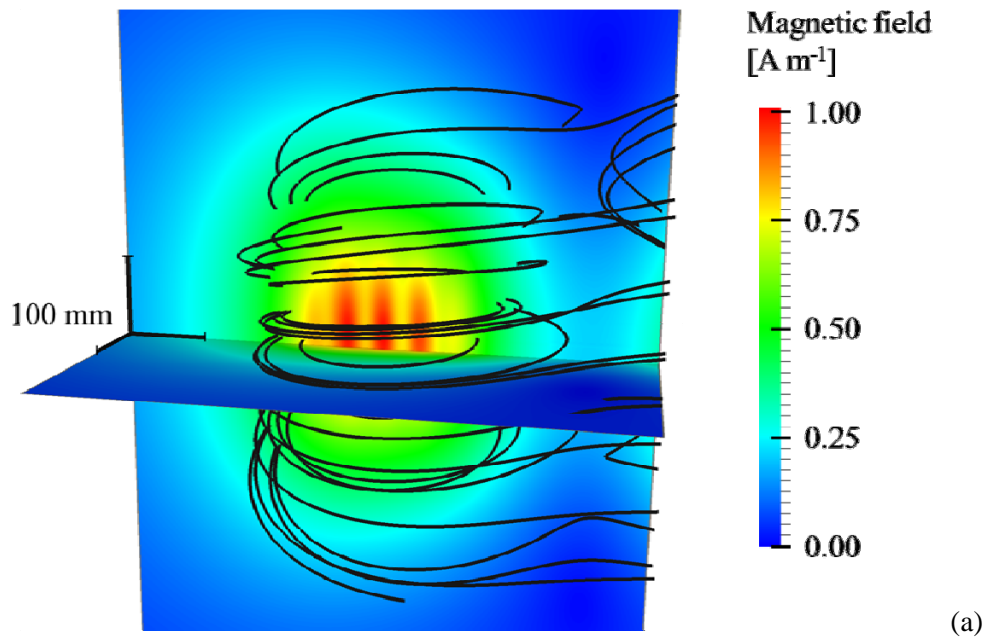


Figure 2. The magnetic field distribution for the odd (a) and even (b) modes for an input power of 1 W. The transmitting coil is located approximately 3 cm behind the observation plane. Streamlines show the direction of the magnetic field.

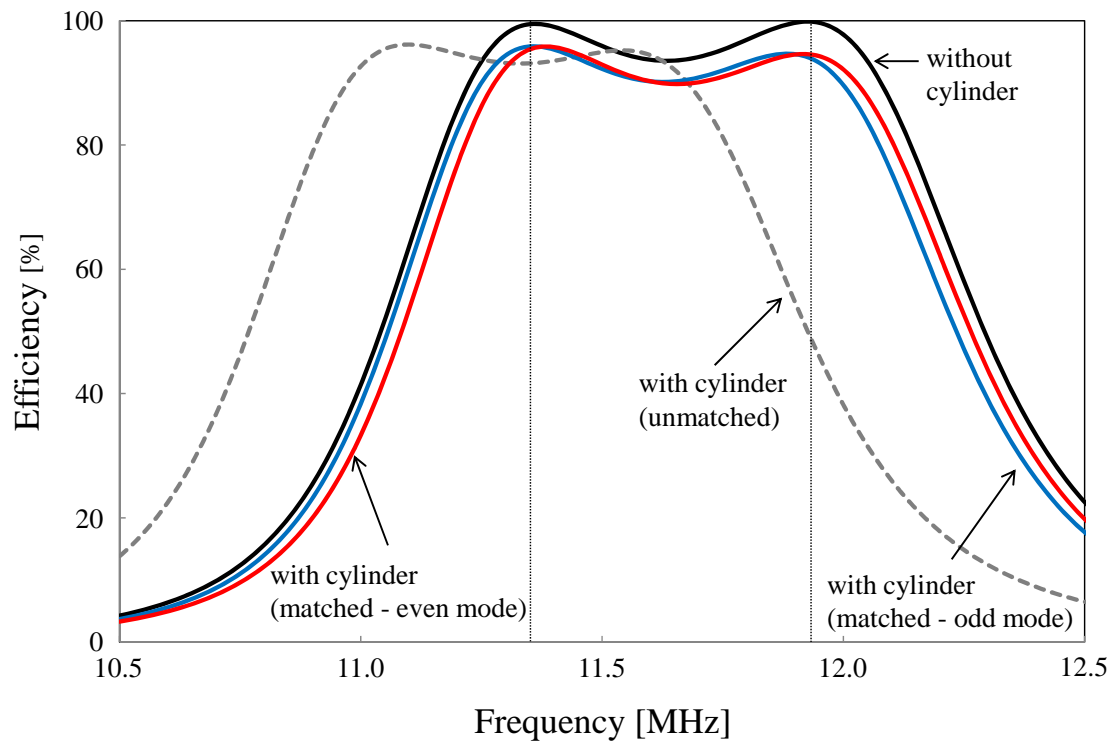


Figure. 3. Power transmission efficiency from the transmitting coil to the receiving coil for the odd and even modes.

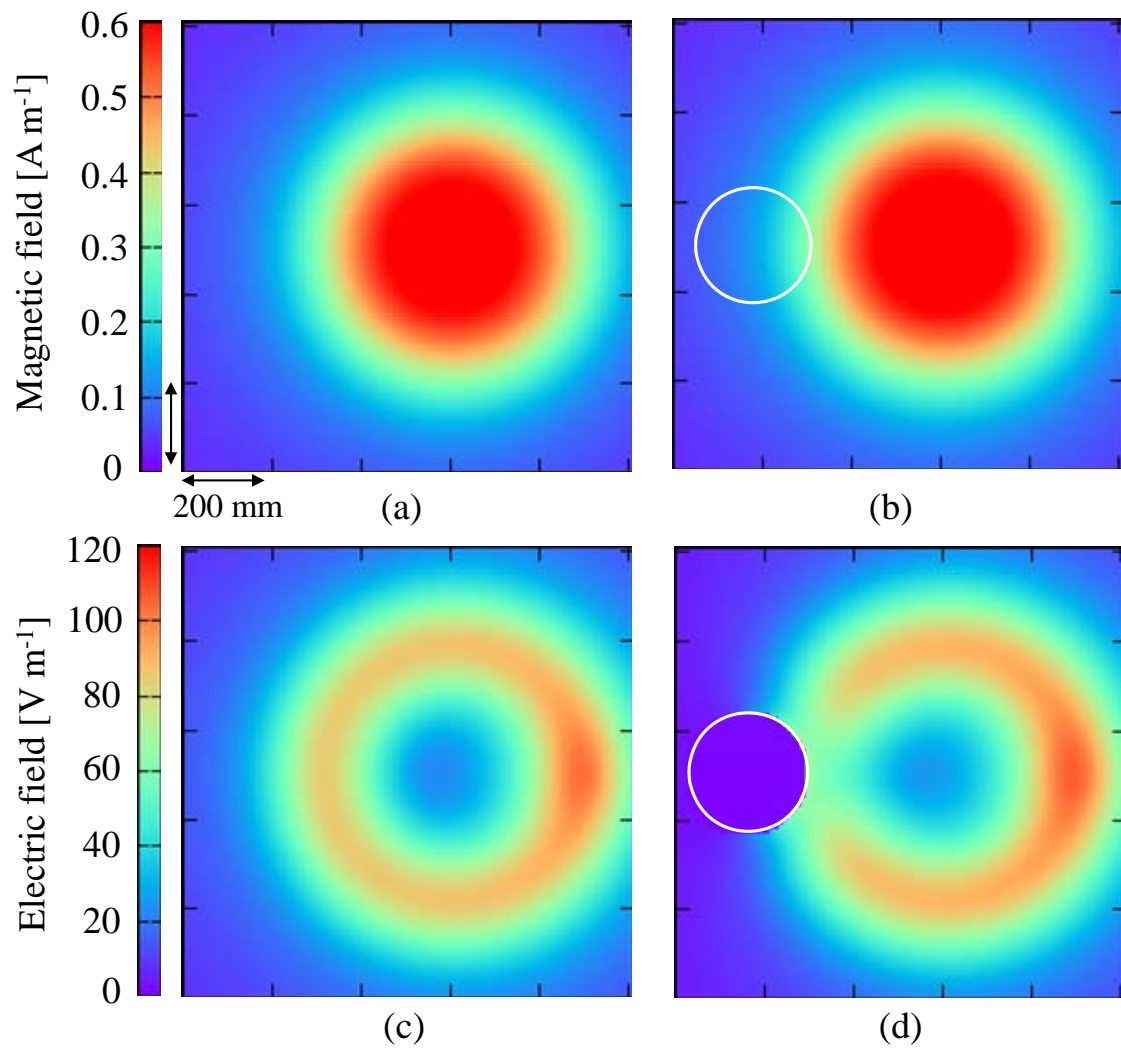


Figure 4. Magnetic field distribution without (a) and with (b) the cylinder and electric field distribution without (c) and with (d) the cylinder for the odd mode on the $z=0$ plane.

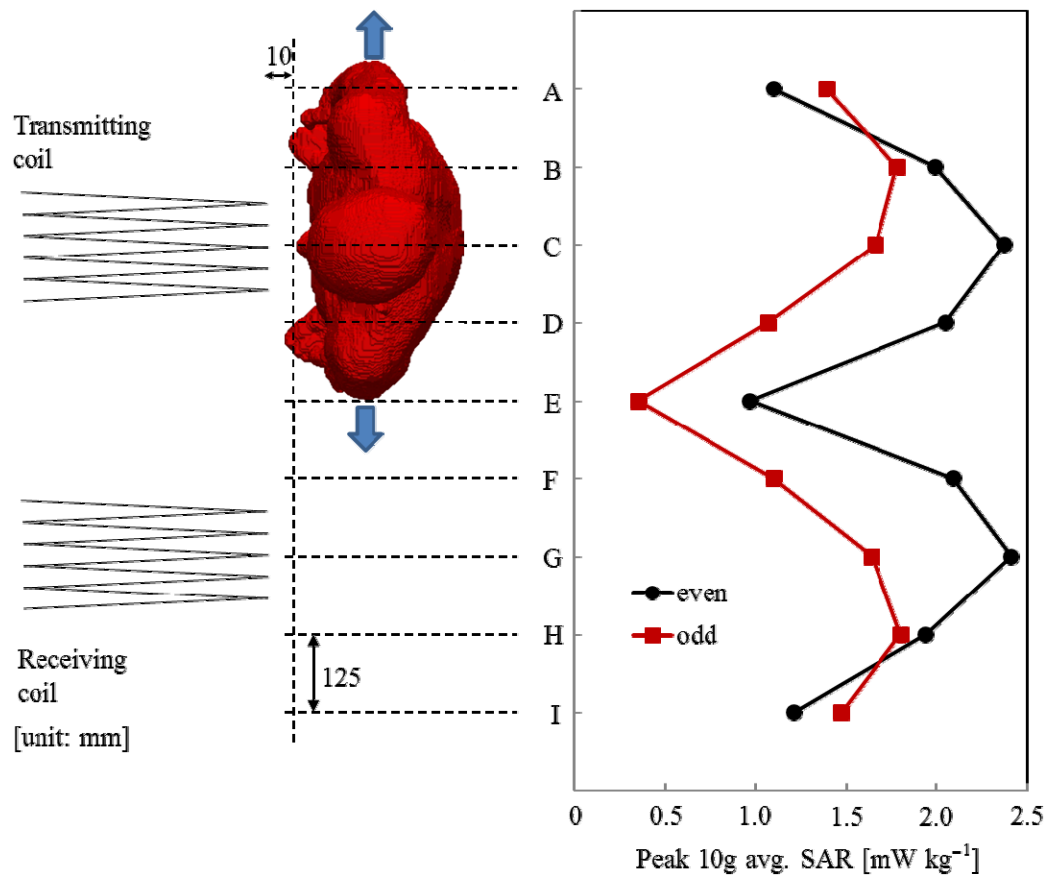


Figure 5. Peak 10 g averaged SAR in the TARO model when the position of the coils is varied laterally. The vertical position of the coils is in front of the chest (corresponding to position D in figure 6), and the horizontal distance between the nose tip of the model and the coils is 10 mm.

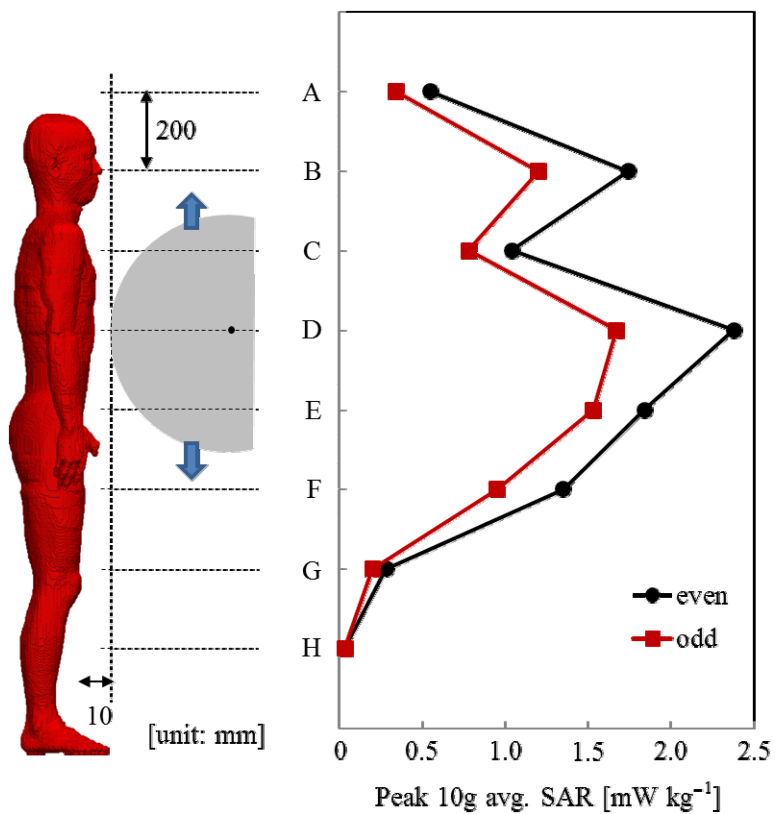


Figure 6. Peak 10 g averaged SAR in the TARO model when the height of the coils is varied.

The lateral position of the coils corresponds to the front of the chest (position C in figure 5).

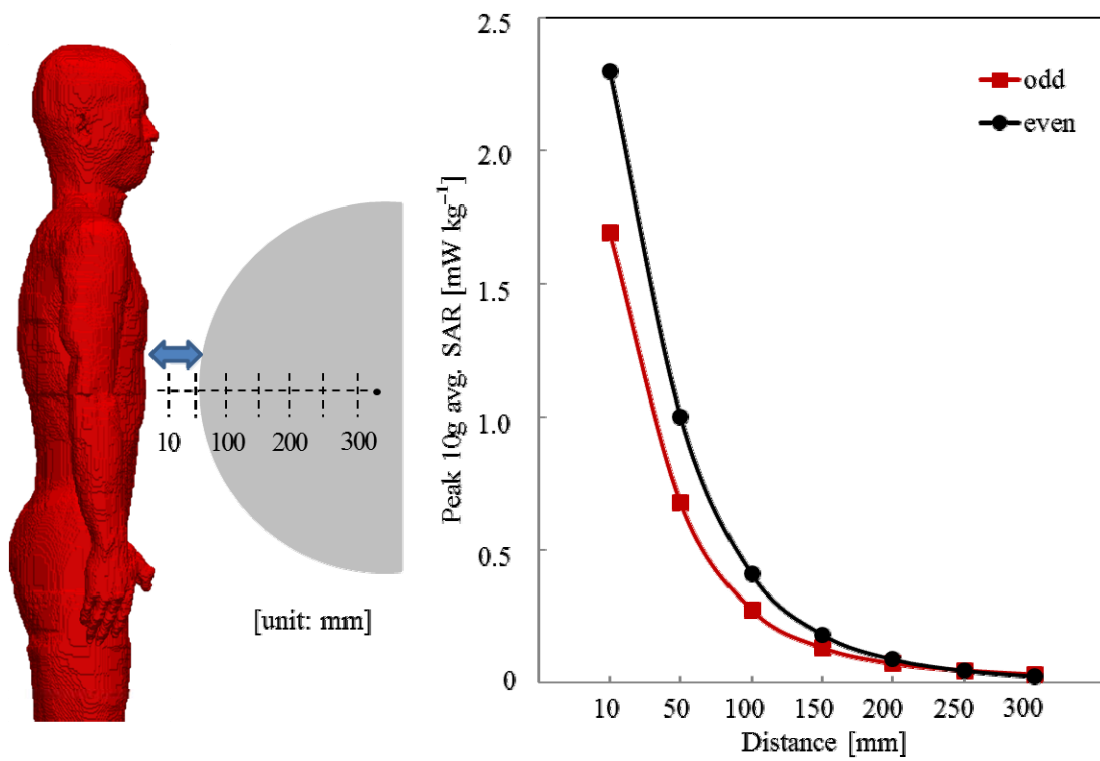


Figure 7. Peak 10 g averaged SAR in the TARO model when the horizontal distance measured from the nose tip to the coils is varied. The vertical and horizontal positions are C and D in figures 5 and 6, respectively.

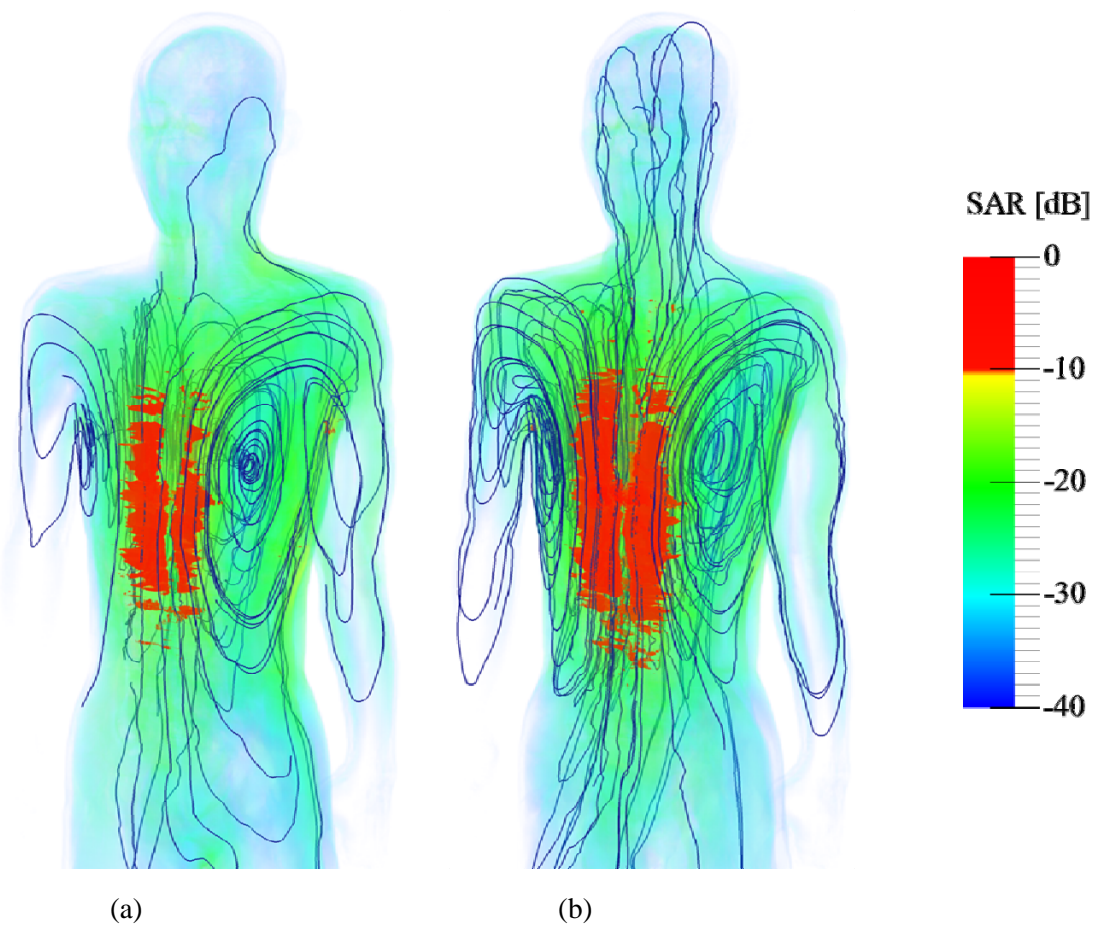


Figure 8. The distribution of the SAR for the odd (a) and even (b) modes with the TARO model located directly in front of the transmitting coil. The SAR of 0 dB corresponds to the maximum pointwise SAR for the even mode. Streamlines show the direction of the induced current.